Observations of Broad-Band Micro-Seisms During Reservoir Stimulation

G.E. Sleefe, N.R. Warpinski, and B.P. Engler, Sandia National Labs*

SUMMARY

During hydrocarbon reservoir stimulations, such as hydraulic fracturing, the cracking and slippage of the formation results in the emission of seismic energy. The objective of this study was to determine the properties of these induced micro-seisms. A hydraulic fracture experiment was performed in the Piceance Basin of Western Colorado to induce and record micro-seismic events. The formation was subjected to four processes; break-down/ballout, step-rate test, KCL mini-fracture, and linear-gel mini-fracture. Micro-seisms were acquired with an advanced three-component wall-locked seismic accelerometer package, placed in an observation well 211 ft offset from the fracture well. During the two hours of formation treatment, more than 1200 micro-seisms with signal-to-noise ratios in excess of 20 dB were observed. The observed micro- seisms had a nominally flat frequency spectrum from 100 Hz to 1500 Hz and lack the spurious tool-resonance effects evident in previous attempts to measure micro-seisms. Both p-wave and s-wave arrivals are clearly evident in the data set, and hodogram analysis yielded coherent estimates of the event locations. This paper describes the characteristics of the observed micro- seismic events (event occurrence, signal-to-noise ratios, and bandwidth) and illustrates that the new acquisition approach results in enhanced detectability and event location resolution.

INTRODUCTION

It has long been recognized that reservoir stimulations such as hydraulic fracturing result in the emission of seismic energy [1]. A popular methodology is to place one or more seismic sensors in either the stimulation well or an adjacent monitoring well to determine the origin of the micro-seismic events. Typically, a wall-locking three-component geophone instrument is utilized to sample the vector wave-field produced by the micro-seism. The data from the three geophones is then processed such that the particle motion polarization is used to infer the orientation of the fracture plane [2]. In order to utilize the polarization approach, however, the seismic receiver instrument must faithfully record the particle motion of the seismic wave-field that is incident on the borehole. The conventional wall-locking geophone instrument generally does not enable the accurate measurement of particle motion over a wide frequency range [3]. Two instrument limitations can cause the wall-locked geophone to record inaccurate particle motions. The first limitation, known as locking resonance, results from inadequate coupling of the geophones to the borehole over a wide frequency band. The locking arm of the instrument provides good coupling of the geophones to the borehole only at relatively low frequencies. At some higher frequency, the motions of the clamping unit do not follow the motions of the borehole wall. In conventional VSP geophone receivers, the resonant frequency of the clamped receiver is typically in the 200 Hz to 400 Hz range. Therefore, conventional VSP instruments can only be used for accurate polarization measurements for seismic excitations below about 200 Hz. Methods for extending the frequency range above this limit include the use of novel clamping packages or geophones cemented directly to the formation. The second limitation in using the polarization method is that the geophone itself often does not accurately measure particle motion over a wide frequency range. Conventional geophones exhibit spurious modes which are due to off-axis excitation of the geophone springs. The spurious mode manifests itself as a resonance effect which occurs at a frequency which is approximately 25 times higher than the natural frequency of the geophone. For example, a 10 Hz geophone can exhibit spurious modes at and above 250 Hz, thus limiting its usefulness above 250 Hz. Additional geophone limitations include phase shifts within the first few octaves above the natural frequency and high-frequency self-noise above approximately 200 Hz [4].

Due to the limitations presented by the conventional wall-locking geophone, an advanced borehole seismic receiver was utilized to extend the useable frequency range out to 1500 Hz. The advanced receiver utilizes a novel clamp mechanism which enables its resonant frequency to be above 2000 Hz. Additionally, solid-state accelerometers are used as the sensing device, thereby eliminating spurious modes, phase errors, and high frequency noise limitations. The resulting seismic receiver is potentially capable of accurate particle motion measurement to frequencies nearly an order of magnitude higher than previously reported. This suggests that much improved detection and location of micro-seismic events can be obtained to map a hydraulic fracture. The remainder of this paper will describe an experiment in which a broadband accelerometer-based seismic receiver was used to measure micro-seisms generated by hydraulic fracture treatments. The resulting data described below depict the advantages of broadband micro-seism measurements.

DATA ACQUISITION APPROACH

The borehole seismic receiver utilized in the experiments is the accelerometer-based Advanced Borehole Receiver, available from OYO Geospace Corp., Houston, TX [4]. The receiver consists of two pressure housings fitted with standard Gearhart-Owens seven conductor cable-heads, one on either end of the clamping section. One housing contains the tri-axially arranged accelerometers and the other housing contains the electric gear-motor assembly. This gear-motor drives the rectangular piston perpendicular to the longitudinal axis of the tool through the use of a 1:1 right angle gearbox to clamp the tool into the borehole.

Finite element analysis of the receiver was performed to assure that the clamping mechanism has a potential flat frequency response out to 2.0 KHz. The analysis resulted in a clamping piston design with 1.5 inches of travel, and accommodation of adapters to allow for clamping into boreholes ranging from 4.25 inches to 9 inches in diameter. The clamp force to tool weight ratio developed by this design is a function of the gearset selected to mate with the electric motor, and can vary from 5:1 to 20:1.

The low-noise piezo-electric accelerometers utilized in the receiver offer significant advantages over conventional geophones. These accelerometers do not exhibit the spurious resonance problem common to geophones, are not sensitive to their mounting

orientation, and most importantly are more sensitive than geophones above 150 Hz. The specifications for these unique borehole accelerometers were developed by Sandia and resulted in a custom sensor which is now available from Wilcoxon Research as model 731-20.

The standard Gearhart-Owens seven conductor interface allowed each accelerometer to use one pair of conductors with the motor using the center conductor and armor for electrical connection. With ground established at the tool, the accelerometers electrically isolated, and the armor at ground potential, battery operated constant current power supplies uphole eliminated 60 Hz interference on the 12000 ft wireline. The power supplies provide 20 dB of amplification in addition to the downhole preamplification of 30 dB.

The analog accelerometer signals from the uphole preamplifier were directly digitized for subsequent analysis. For the perforation orientation shots (described below), the signals were digitized by an EG&G 2420 seismograph at a sample rate of 4000 samples per second. For recording micro-seisms during the hydraulic fracture experiment, continuous digital recording of the data was required. The accelerometer signals were continuously digitized and stored on a Sony model PC208 8-channel Digital Audio Tape (DAT) recorder at a sample rate of 12000 samples per second per channel. The DAT equipment was particularly well suited for this application since the signals are sampled simultaneously on all channels with a dynamic range of 85 dB, with each standard DAT tape capable of recording continuously for 3 hours. The digital data from the DAT can either be directly downloaded into a Personal Computer for further analysis, or redigitized by another recorder (if higher sample rates were desired). The data presented in this paper were redigitized by an EG&G 2401 seismograph at a rate of 20000 samples per second and were directly analyzed on the PC. Analysis of the digital seismic data was performed on a Compaq/486 system running both MicroMax software and Sandia-developed micro-seismic analysis software.

HYDRAULIC FRACTURE EXPERIMENT

A hydraulic fracture experiment was undertaken for the purposes of generating and measuring micro-seismic events. The experimental site is located near Rifle, CO in the Piceance basin and is referred to as the joint DOE/GRI M-Site. The overall objective was to perform a limited site-suitability test to determine if the site had the necessary qualities for further development as a full-scale instrumented facility for mapping and modeling hydraulic fractures. In the test described herein, only one seismic receiver was used in a single offset well to determine if the downhole conditions are suitable for seismic instrumentation and if sufficient micro-seisms are generated during hydraulic fracturing to provide accurate maps of the fractures.

A site schematic is shown in Figure 1. The three-component accelerometer receiver was placed in well MWX-2 at a depth of 4881 ft, 211 ft south of the treatment well, MWX-3. To assure good coupling of the receiver to the scaled and corroding steel-casing, the receiver was clamped with approximately 50 lbs of force, then slowly dragged up the hole while increasing the clamp force to 150 lbs. This assured that the receiver was centered in the hole and that minimal scaling remained between the clamp arm and the casing. Once the receiver was locked in at 4881 ft, its orientation was determined from the detonation of charges in MWX-3. Ten decoupled 3.5 gm perforation charges were detonated and the recorded seismic signals were utilized to determine the absolute orientation of the receiver. The polarization method (often referred to as the hodogram method) was applied to the first 1.5 cycles of the p- wave arrival to determine the receiver orientation.

The first monitoring experiment was performed during the week of September 21, 1992, and focused on the collection of background noise measurements and the collection of cross-well perforation shot data. The hydraulic fracturing of the formation and micro-seismic monitoring tests were conducted the week of October 12, 1992. Well MWX-3 was first perforated from 4900 ft to 4946 ft and subsequently treated in four separate operations; breakdown, step-rate test, KCL mini-frac, and linear gel mini-frac. Seismic data were recorded continuously during all four injections. The injection volumes and flow rates are summarized in Table 1. The variations in the injection parameters were due to other site objectives, such as determining the closure stress and performing fracture modeling. Detailed down-hole pressure and surface flow- rate measurements were gathered continuously during the injections for later correlation with the seismic data.

Table 1 Injection data

TEST	DATE	VOLUME	RATE	FLUID
BREAKDOWN	10/14/92	70 bbl	8 bpm MAX	40# X-LINK GEL
STEP-RATE	10/14/92	100 bbl	20 bpm MAX	KCl
KCl MINIFRAC	10/14/92	304 bbl	30 bpm MAX	KCl
GEL MINIFRAC	10/15/92	634 bbl	25 bpm MAX	40# LINEAR GEL

RESULTS AND DATA ANALYSIS

Even though the seismic monitoring well is situated near active producing gas wells, it was found that the background seismic noise level was particularly low. The nominal background noise was -150 dB relative to 1 g/$\sqrt{Hz}$ (1 g = 9.8 m/sec/sec) at frequencies between 70 Hz and 400 Hz, and decreased to -160 dB at and above 1000 Hz. This low noise floor is an attribute of the extremely low electronic self-noise of the accelerometers, and enabled the detection of even the weakest broad-band events. The rms background noise was primarily dominated by low frequency cultural phenomena and ranged from 1 - 4 micro-g rms. To determine the number of events recorded during the injections, the accelerometer signals were peak-detected at a threshold of 40 micro-g, and the number of detected events were counted. Note that the peak-detector counter counts the number of events with signal-to-noise ratios of at least 10:1. In all, more than 1200 micro-seismic events were counted in this manner during the two hours of injection and shut-ins. Figure 2 displays a histogram of the number of significant events occurring during the gel mini-frac experiment. It is seen in Figure 2 that the seismic activity, i.e. the generation of fracture-induced micro-seisms, correlates with the resulting treatment-well pressures.

In order to determine the useful bandwidth of the micro-seismic events, Fourier spectra were computed from the raw accelerometer signals. Results of spectral averaging of 256 detected events (those with peak amplitude greater than 40 micro-g) during the gel mini-frac are displayed in Figure 3. The spectral content is provided for each of the three accelerometers in the downhole receiver, and for reference, the measured seismic noise floor is plotted. It is clear from Figure 3 that excellent signal-to-noise is available throughout the measurement frequency band of 100 Hz to 1500 Hz. At frequencies below 100 Hz, ambient background noise

becomes comparable to the micro-seismic signal strength. Above 1500 Hz, resonances in the clamped accelerometer package and the accelerometers themselves begin to affect the coherency of the three components. Noting that the spectral content of all three accelerometer signals is comparable in the 100 Hz to 1500 Hz range, we conclude that this entire bandwidth is free of resonance effects and can be used in the polarization analysis.

A plot of a typical micro-seismic event is depicted in Figure 4. Note the clear delineation of both the p-wave and s-wave arrivals. For this event, the spectra for both the micro-seismic event and the pre-event noise are plotted in Figure 5. Note that for this event, the majority of energy in the micro-seism event is at frequencies above 250 Hz. This result confirms the need for broadband measurement of the micro-seismic events.

The three accelerometer signals of Figure 4 are over-plotted in Figure 6a. The overlay indicates that during the p-wave arrival, all three accelerometers are in-phase, i.e. that the particle motion in essentially linearly polarized. The majority of micro-seisms recorded during this experiment exhibit this feature, implying that the polarization approach is appropriate. Figures 6b and 6c plot the hodogram for the event of Figure 6a. The hodograms enable determination of the orientation of the origin of the micro-seismic event relative to the receiver. By measuring the time delay between the p and s arrivals, and using the known seismic velocities in the formation, a range estimate of the event origin may also be formulated. A group of 67 significant micro-seismic events were analyzed in this fashion to determine the origin of seismic events during the hydraulic fracture experiment. A map of the event location estimates is provided in Figure 7. Also shown in Figure 7 is the orientation of the known stress field at this site. Since the net estimated orientation of the event locations are consistent with the known stress fields, this technique may prove valuable in hydraulic fracture diagnostics.

CONCLUSIONS

During a hydraulic fracture experiment in the Piceance Basin of Western Colorado, significant micro-seismic activity was recorded in an offset monitoring well. The micro-seisms were acquired with a novel three-component wall-locked seismic accelerometer package, and enabled enhanced detection of micro-seismic events. During the two hours of formation treatment, more than 1200 micro-seisms with signal-to-noise ratios in excess of 20 dB were observed. Micro- seismic event activity was directly correlated with the induced borehole pressures in the treatment well. The observed micro-seisms had a nominally flat frequency spectrum from 100 Hz to 1500 Hz and lacked the spurious tool-resonance effects evident in previous attempts to measure micro-seisms. The recorded micro-seisms exhibited discernable p and s wave arrivals, and good coherency was obtained from all three components of the p-wave arrival. Using polarization analysis and p-to-s wave travel time differences, estimates of the micro-seismic event location were obtained. The estimated origin of the micro-seismic events correlated well with the known stress field in the formation.

ACKNOWLEDGEMENTS

This project was funded by the Gas Research Institute under contract number 5089-211- 2059, managed by Steve Wolhart. The authors would like to thank Steve for his help and acknowledge the able field support provided by Rich Peterson, Paul Branagan, Mike Middlebrook, and Roy Wilmer of CER Corporation.

REFERENCES

1. Dobecki, T.L., "Hydraulic Fracture Orientation Using Passive Borehole Seismics, "SPE 12110, 58th SPE Annual Technical Conference, San Francisco, CA, October 5-8, 1983.

2. Sorrells, G.G., and Mulcahy, C.C., "Advances in the Microseism Method of Hydraulic Fracture Azimuth Estimation, " SPE 15216, Proceedings, SPE Unconventional Gas Technology Symposium, Louisville, KY, pp. 109-120, May 18-21, 1986.

3. Galperin, E.I., "Vertical Seismic Profiling and its Exploration Potential," D. Reidel Publ. Co., Boston, MA, pp. 25-26, 1985.

4. Sleefe, G.E., and Engler, B.P., "Experimental Study of an Advanced Three-Component Borehole Seismic Receiver," Proceedings, 61st Annual SEG Meeting, Houston, TX, pp. 30-33, 1991.

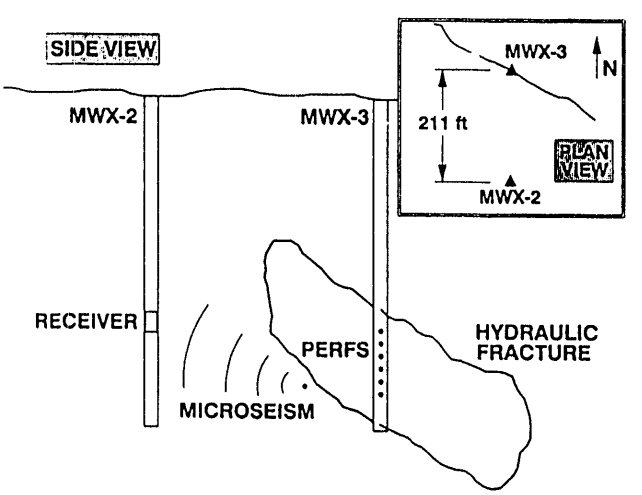

Figure 1 - Site schematic and plan view (insert)

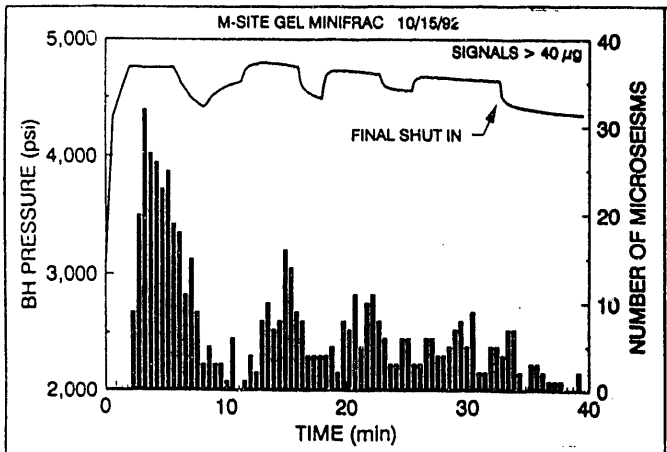

Figure 2 - Histogram of micro-seisms detected during the gel minifrac correlated with bottom-hole pressure

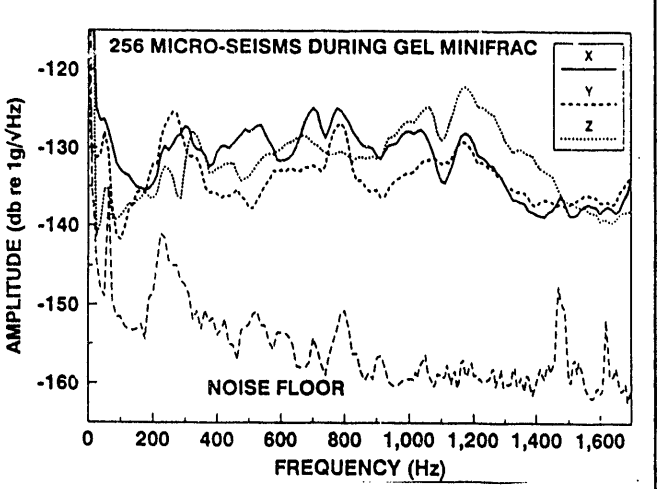

Figure 3 - Average spectra of 256 events detected during the gel minifrac compared with the measured noise floor

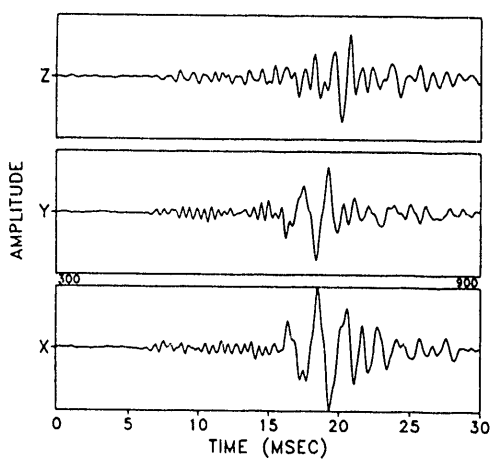

Figure 4 - Example micro-seismic event (MS34)

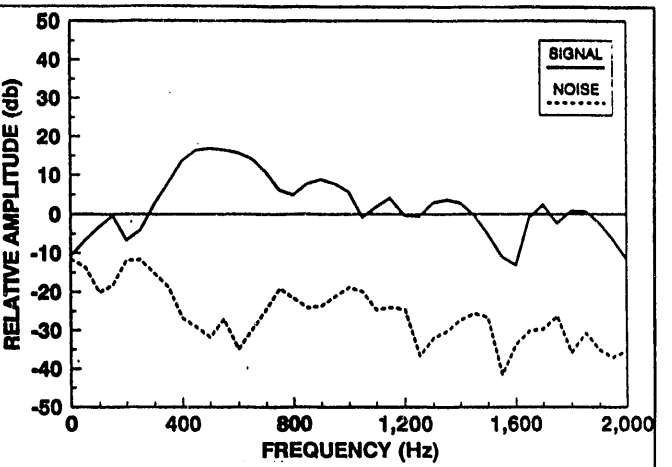

Figure 5 - Spectra of event and pre-event noise

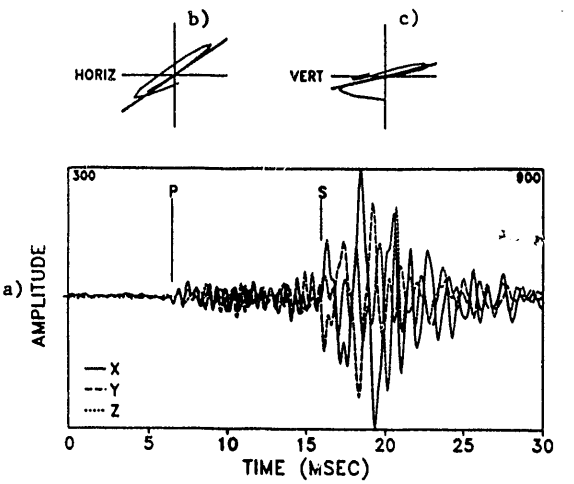

Figure 6 - a) Overplot of micro-seismic event MS34; b) horizontal-plane hodogram; c) vertical-plane hodogram

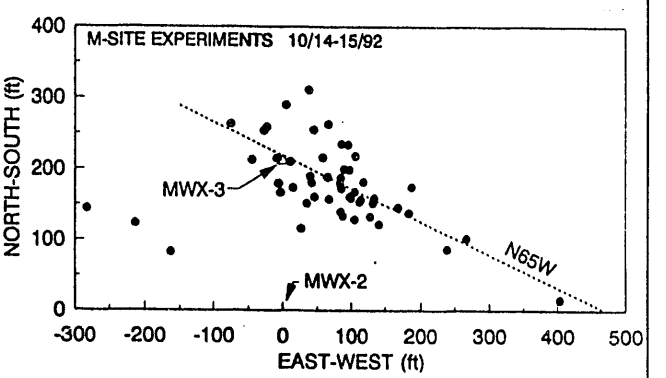

Figure 7 - Plan view of micro-seism event locations

DATE
FILMED
8/17/93